Original Research Article

FGFR1 Signaling is Associated with the Magnitude of Morphological Integration in Human Head Shape

TÁBITA HÜNEMEIER,[1] JORGE GÓMEZ-VALDÉS,[2] SOLEDAD DE AZEVEDO,[3] MIRSHA QUINTO-SÁNCHEZ,[3] LUCIANE PASSAGLIA,[1] FRANCISCO M. SALZANO,[1] GABRIELA SÁNCHEZ-MEJORADA,[2] VÍCTOR ACUÑA ALONZO,[4] NEUS MARTÍNEZ-ABADÍAS,[5] MARIA-CÁTIRA BORTOLINI,[1†] AND ROLANDO GONZÁLEZ-JOSÉ[3†*]

[1]*Departamento de Genética, Instituto de Biociências, Universidade Federal do Rio Grande do Sul. Caixa Postal 15053, 91501-970 Porto Alegre, RS, Brazil*

[2]*Departamento de Anatomía, Facultad de Medicina, Universidad Nacional Autónoma de México, Circuito Interior, Ciudad Universitaria, 04510 Distrito Federal, México*

[3]*Centro Nacional Patagónico-CONICET, Bvd. Brown 2915, U9120ACD, Puerto Madryn, Argentina*

[4]*Escuela Nacional de Antropología e Historia, México, DF, México*

[5]*EMBL-CRG Systems Biology Research Unit, Center for Genomic Regulation (CRG), Dr. Aiguader 88, 08003, Barcelona, Spain*

ABSTRACT: Objectives: The head can be used as a model to study complex phenotypes controlled simultaneously by morphological integration (MI) due to common factors, and modular patterns caused by local factors affecting the development and functional demands of specific structures. The fibroblast growth factor and receptor system (FGF/FGFR) participates in cell communication and pattern formation in osseous tissues, among others, and there is compelling evidence from mouse model studies suggesting a role of the FGF/FGFR pathway as a covariance-generating signaling process in head development. Here we use human data to test if specific genetic variants of another gene of this pathway, the FGFR1 gene, can be associated with differences in the integration of the head.

Methods: We explored whether and how three specific variants on FGFR1, previously associated with human cephalic index, influence the pattern and level of head integration of one Native American and one admixed group from Mexico. MI, measured as the intensity of covariation among head traits, was assessed using data from three-dimensional head landmark coordinates taken on 176 individuals.

Results: Individuals carrying the derived allele of the rs4647905:G>C polymorphism present significantly greater levels of head MI, especially in facial structures and on the shape space where the modular portion of the covariation is explicitly removed.

Conclusions: Since *FGFR* genes present nonconservative and tissue-specific splicing sites, they may have some effect on protein structure and performance likely involved in developmental processes responsible for the magnitude and pattern of MI in the human head. Am. J. Hum. Biol. 00:000–000, 2013.

The human head can be used as a model to study complex phenotypes whose "genotype-phenotype map" (Wagner and Altenberg, 1996) is influenced simultaneously by integration and modularity patterns (Hallgrímsson et al., 2009; Lieberman, 2011; Mitteroecker and Bookstein, 2007). Morphological integration (MI) refers to the coordinated variation of two or more characters that reflects common function and/or development (Cheverud, 1982, 1984, 1995, 1996; Hallgrímsson et al., 2009; Olson and Miller, 1958; Willmore et al., 2007), and it is expressed through the statistical covariation between traits. MI assumes that functionally and/or developmentally related traits will be coinherited and will produce coordinate responses to evolution (Cheverud, 1982, 1984, 1995, 1996; Olson and Miller, 1958). Cheverud (1996) distinguished three MI dimensions. First, functional/developmental integration refers to the interaction of morphological elements in the performance of some function or developmental process. Second, genetic integration, represented by the covariance structure of the phenotype, refers to the common inheritance of traits arising from linkage disequilibrium or pleiotropy. Finally, integration is manifested at the evolutionary level, by the coordinate evolution of elements contained within functional complexes. These three forms of MI are linked (Cheverud, 1996) and play a key role in the evolution of complex morphological structures. MI can operate as constraints that facilitate evolution on some particular directions of the morphospace, while limiting variation in other directions (Schluter, 1996). In other words, evolutionary change is more likely to occur in some specific directions (the so-called lines of least evolutionary resistance) than in others (Martínez-Abadías et al., 2012; Schluter, 1996). Previous works focusing on skull integration patterns, indicated that these patterns have been stable across placental mammals (Goswami, 2006; Porto et al., 2008), New World primates (Marroig and Cheverud, 2001), and modern human populations (González-José et al., 2004), and that the shared pattern

Additional Supporting Information may be found in the online version of this article.

Contract grant sponsor: Argentina: Consejo Nacional de Investigaciones Científicas y Técnicas. CONICET; Brazil: Conselho Nacional de Desenvolvimento Científico e Tecnológico (CNPq), Coordenação de Aperfeiçoamento de Pessoal de Nível Superior (CAPES) and Fundação de Amparo à Pesquisa do Estado do Rio Grande do Sul (Programa de Apoio a Núcleos de Excelência).

†These authors contributed equally to this work and should be considered as joint last authors.

*Correspondence to: Rolando González-José, Centro Nacional Patagónico-CONICET, Bvd. Brown 2915, U9120ACD Puerto Madryn, Argentina. E-mail: rolando@cenpat.edu.ar

Received 16 May 2013; Revision received 24 November 2013; Accepted 26 November 2013

DOI: 10.1002/ajhb.22496
Published online 00 Month 2013 in Wiley Online Library (wileyonlinelibrary.com).

of skull covariation can be preserved even under genetic and developmental alterations (Hallgrímsson et al., 2007, 2009; Martínez-Abadías et al., 2011), disease (Richtsmeier and Deleon, 2009), and cultural deformation practices (Martínez-Abadías et al., 2009).

Integration patterns, however, are not homogeneous across the constitutive parts of a complex phenotype. There are sets of more tightly integrated traits, called modules, which are poorly integrated among them and relatively independent of one another (Klingenberg, 2008; Raff, 1996). Modularity thus refers to the division of developmental systems into partially dissociated components that are themselves integrated. A strict definition of module from the evolutionary biology standpoint entails that a set of morphological characters, which collectively accomplish a particular function, are tightly integrated by strong pleiotropic genes, and maintain a relative independence from other modules. Thus, a modular genotype–phenotype map can be decomposed into several independent and more local genotype–phenotype maps with fewer pleiotropic effects among the modules (Mitteroecker and Bookstein, 2008). An important characteristic of a modular genotype–phenotype map is that it enhances the ability of the genetic system to generate adaptive variants. In consequence, both integration and modularity are key determinants of evolvability since they facilitate rapid evolution due to canalization of pervasively integrated traits, as well as simultaneous independent response to selection avoiding "side-effects" (Griswold, 2006; Hallgrímsson et al., 2009; Hansen and Houle, 2008; Raff and Sly, 2000).

Mitteroecker and Bookstein (2007, 2008) postulated a formal model to account for the integrated/modular nature of the genotype–phenotype map of complex structures that discriminates among common and local developmental factors that differently affect phenotypic variables. In an attempt to formalize the factor model devised by Wagner and Altenberg (1996), these authors developed a model of common and local factors that differently affect morphometric variables. In this approach, morphometric modules can be defined as sets of variables with some amount (non-zero) of within-module covariances, even when the covariances due to common factors have been removed. Thus, in these sets of variables, the residual between-module covariances are all near zero (Mitteroecker and Bookstein, 2007). In their model, "local factors" such as developmental processes, functional properties, and tissue-specific expression or reception patterns tend to contribute to morphological variation within one module only. Conversely, major developmental genes and gene families (e.g., *SHH*, *FGF*, *BMP*, *GH*/*IGF*) with pleiotropic effects affecting traits across different modules configure what they denominate "common factors." In this way, the factor model separates the full shape space on an integrated space, defined by the common factors (i.e., the dimensions of shape variation that are integrated between the a priori modules), and on the modular space, the space defined by local factors, reflecting those shape changes that remain after removing the effect of the common factors.

In this context, understanding how particular signaling systems generate specific covariation patterns, or modulate the magnitude of integration, is of key importance to disentangle the determinants of phenotypic covariation.

Role of FGF/FGFR *pathway in the head genotype–phenotype map*

Interaction between epithelial and mesenchymal cells is vital to the normal development of almost all developmental systems. Over the last decade, the identification of mutations in fibroblast growth factors (*FGFs*) and their receptors (*FGFRs*) has demonstrated that these genes play a critical role in epithelial–mesenchymal interactions regulating the development of many tissues within the head, as the craniofacial skeleton (Dorey and Amaya, 2010; Ornitz and Itoh, 2001). The crucial role of the FGF/FGFR signaling system in the development of the skull, and thus the vertebrate head, has been highlighted by the discovery that many human congenital craniosynostosis syndromes characterized by premature closure of cranial sutures, dysmorphic skulls, facial, and brain malformations, such as Apert, Pfeiffer, Crouzon, Muenke, Jackson-Weiss, and Beare-Stevenson, are caused by mutations in genes of the *FGF*/*FGFR* pathway, including *FGFR1, 2*, and *3* (Hajihosseini et al., 2009; Robin et al., 1998). Further evidence of the general role of FGF/FGFR signaling pathway on head development is the finding that, phenotypically, craniosynostosis syndromes can be divided into different categories on the basis of the affected functional domain of the protein rather than on the type of FGFR (Cunningham et al., 2008).

In craniofacial skeletogenesis, the FGF signaling pathway participates in suture and synchondrosis regulation (Nie et al., 2006), as well as in facial, cranial vault and cranial base development (Szabo-Rogers et al., 2010). Research on mouse models of Apert and Crouzon syndrome has shown that besides premature suture fusion, midfacial hypoplasia and cleft palate, which are characteristic traits of craniosynostosis syndromes, mouse models carrying *Fgfr2* mutations also present altered MI patterns within the skull and between the skull and non-osseous structures of the head (Martínez-Abadías et al., 2011, 2013). Thus, *FGFs* and *FGFRs* and their orthologs are proper candidates to study complex genotype–phenotype interaction networks where MI and modularity patterns operate simultaneously to coordinate the proper development of the head.

Here, we focus on the *FGFR1* gene (MIM# 136350), located at 8p11.2–p11.1, which contains 19 exons spanning 55 kb and has at least nine known isoforms. It is a cell surface receptor that signals via two major transduction pathways: Ras/mitogen-activated protein kinase and PLCγ pathways (Groth and Lardelli, 2002). Molecular studies have demonstrated that alternative splicing of *FGFR1*modifies both extracellular and intracellular domains of this receptor, resulting in forms that vary in their affinity and ligand-binding specificity for fibroblast growth factor (Bruno et al., 2004; Jin et al., 1999). Mutations in *FGFR1* have also been reported to affect the timing of calvarial suture fusion resulting in craniosynostosis and facial abnormalities, such as in Pfeiffer syndrome type 1 (Robin et al., 2008).

Regarding genotype–phenotype relationships on *FGFR1* normal variation, Cousens and Dall (2005) showed that the allele C at *FGFR1* rs4647905:G>C polymorphism is associated with a decrease in the cephalic index (CI). On a recent article, we reported a tendency for a decrease in CI in individuals homozygous for the allele C in admixed and Native American populations, as well

as a statistically significant association between *FGFR1* rs3213849:G>A polymorphism and CI when both populations were pooled (Gómez-Valdés et al., 2013). We also showed that these polymorphisms are mainly related to the length of the head vault: individuals carrying the derived alleles in both sites exhibit head lengths dramatically increased in the antero-posterior axis, especially among the admixed sample (Gómez-Valdés et al., 2013).

Considering the pervasive nature of the MI that characterizes the human skull (Martínez-Abadías et al., 2012), it is likely that the observed association between the CI and the derived alleles of *FGFR1* (Gómez-Valdés et al., 2013), particularly rs4647905:G>C, could involve other cephalometric traits, as well as the overall integration pattern of the head.

Hypotheses about the specific role of FGFR1 *variants in head development*

Here we expand our previous study (Gómez-Valdés et al., 2013) to detect if specific variants of the *FGFR1* gene are associated with significant differences in head shape, patterns, and magnitude of MI between the human face and head vault. The vertebrate skull can be seen as a hierarchically nested integrated structure (Willmore et al., 2006, 2007), where many modules of varying relevance can be hypothesized. Indeed, the functional matrix hypothesis by Moss and Young (1960) proposed that cranial traits that shared functional demands or developmental histories are predicted to show strong covariation or, in other words, constitute modular structures. However, the two higher levels of parcellation proposed for the skull are the face and the neurocranium (Esteve-Altava et al., 2013). In this study, our developmental modules follow what has been termed the "tissue origin" model, whereby it is hypothesized that skeletal structures derived from neural crest cells should covary, and skeletal traits derived from paraxial mesoderm (either somitic or somitomeric) will covary (Zelditch, 1988; Willmore et al., 2006). We used the divisions outlined by Jiang et al. (2002) in which the frontal bone, entire viscerocranium, and the squamous regions are derived from the neural crest, and the nonsquamous portions of the cranial base and cranial vault are of mesodermal origin. Furthermore, note that these skull regions grow during different ontogenic times, and their development is regulated by different epigenetic and genetic factors (Martínez-Abadías et al., 2009). The growth of the neurocranial structures is mainly driven by the growth of the expanding brain, and occurs early during the ontogeny, the prenatal, and neonatal periods, while the face develops later. The face and the mandible grow during a more extended period of time, reaching its maturity once the brain has finished its growth (Sperber, 2001). Moreover, the anatomical separation of the skull into facial skeleton and neurocranium mainly reveals functional interactions within regions (i.e., the facial skeletal morphology develops and responds to visual, olfactory, and masticatory soft tissues and functions, whereas the neurocranium mainly responds to central nervous system growth and vascularization while functioning to protect the brain).

In this context, note that the results obtained by Martínez-Abadías et al. (2011) study on mutant Fgfr2 mice indicate that the face and the neurocranium have a simply structured covariation pattern that can be summarized into a single pair of PLS axes that account for more than 90% of the total covariation. Finally, there are also evolutionary arguments indicating that the face and the neurocranium are the two higher levels in which the modularization of the primate skull can be structured: facial reduction and brain size increase represent general evolutionary trends in hominins (Bastir et al., 2010; Lieberman et al., 2002; Stringer, 2002; Trinkaus, 2003), so they provide an ideal framework for testing integration/modularity hypothesis.

Thus, covariation among the face and the neurocranium can be decomposed into components of magnitude (how strong the general covariation among blocks of traits is) and pattern (which specific parts of one block are prone to covary with parts on the other block). Therefore, the effect of any genetic, environmental, or developmental covariation-generating factor can in turn be dissected into its impact on the pattern and on the magnitude of the covariation. Following this rationale, we test two general null hypotheses. The first null hypothesis tests the assumption that different polymorphisms of the *FGFR1* gene will exhibit nonsignificant differences on the pattern of head MI. The second null hypothesis tests that, independently from the covariation pattern, variants of the *FGFR1* gene will not show differences in the magnitude of head integration. These two general null hypotheses are tested on the full shape space, which informs about shape changes due to the simultaneous effect of common and local factors (Mitteroecker and Bookstein, 2007, 2008).

Since genes like *FGFRs* can be locally expressed and/or pleiotropically shared, based on regulatory rather than coding or splicing mechanisms, the exploration of *FGFR1* variants effects on the integrated versus the modular shape spaces can be of potential interest to illuminate the expression patterns of this gene. In consequence, we further test the two abovementioned null hypotheses on the integrated space, and on the modular space. Finally, we interpret our results in the light of putative splicing events caused by the studied mutations, as well as the concomitant changes on protein structure.

MATERIALS AND METHODS

The sample

Our sample consisted of 176 adult individuals that belong to two populations from central Mexico: Native Totonacos from the Sierra de Puebla region ($n = 78$, 14 males and 64 females) and mestizos from the adjacent cities of Tepango and Mexico ($n = 98$, 39 males and 59 females). All individuals provided written informed consent, and the study was approved by the Faculty of Medicine Research and Ethics Committee of the National Autonomous University of Mexico (Project number 008–2010). Local authorities gave their approval for the study, and a translator was used when needed.

Twenty-six three-dimensional landmark coordinates taken on the face and vault were recorded using a Microscribe G2X digitizer (Immersion Corporation, San Jose, CA) by one of us (JGV). The landmark coverage includes facial and vault external structures accessible on living humans (Fig. 1). Landmark definitions are provided in Supporting Information Table 1. In order to avoid measurement error due to head movements during the digitizing process, a head-supporting device was used to immobilize the head (see Supporting Information Fig. 1).

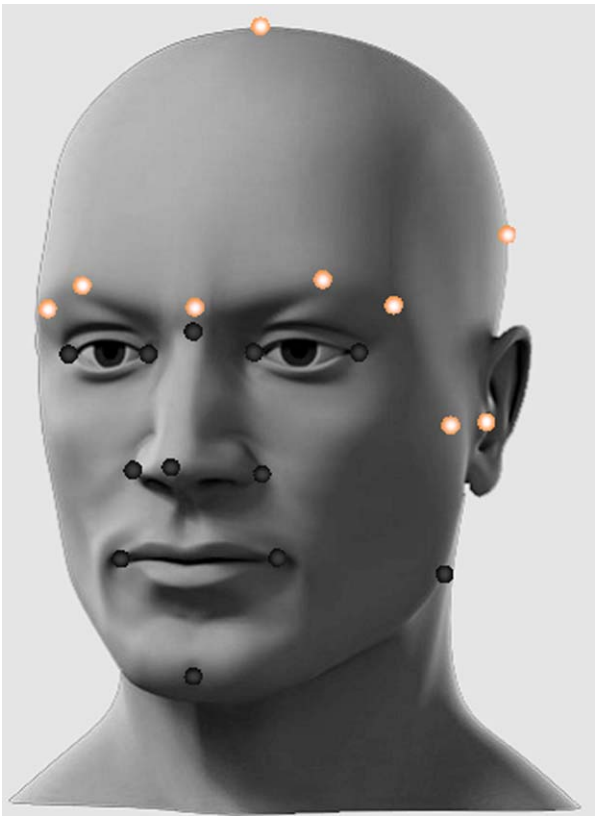

Fig. 1. Mesh representing an adult head showing the landmarks used in this study. Facial landmarks are shown in black, whereas neurocranial landmarks are shown in orange. Some right-side landmarks, as well as opisthocranium, are not visible on this view. [Color figure can be viewed in the online issue, which is available at wileyonlinelibrary.com.]

A repeatability study was carried on to evaluate the technique measurement error (see below).

As covariation patterns recorded on soft-tissue take into account factors that contribute to their variance but do not affect osseous landmarks (e.g., diet, BMI, weight, etc.), the comparison with previous studies based on osseous landmarks should be taken with caution. However, specific studies of variation in soft-tissue thicknesses and their relation to craniometric dimensions obtained significant correlations between many soft-tissue depths and craniometric dimensions. This supports the close correspondence between the amount of soft tissue present on the face and the size of the underlying bony skeleton (Simpson and Henneberg, 2002), and guarantees the reliability of comparisons of the results obtained here with previous, related research made on hard-tissue (bony) structures.

Repeatability analysis

Geometric morphometric methods are based on the analysis of landmark configurations. Soft tissue landmark locations collected from living participants, using calipers or a digitizer, are prone to error, even with the aid of a device that attempts to hold the head steady and special care is given to avoid distortions due to hair thickness.

To examine the proportion among intraindividual (among replicates error) to interindividual differences, the observer collected five observations on a random subsample of six individuals after complete repositioning. Original landmark configurations were superimposed using a Generalized Procrustes Analysis (GPA; Rohlf and Slice, 1990) to place all observations in a common frame of reference and minimize the effects of scale and orientation. The Euclidean distance of each landmark to its respective centroid was computed. For each individual, landmark deviations were calculated relative to the individual landmark mean. Mean deviations and percentage errors were calculated for individual landmarks and subsequently averaged to give a mean deviation and percentage error for each individual across all landmarks (Singleton, 2002). One-way analysis of variance (ANOVA) was conducted for each landmark by individual, and the root mean squares (RMSE) were examined. In the context of this analysis, the root of the within-groups mean squares (root mean square error) corresponds to intraindividual error (Sokal and Rohlf, 1995), while the root of between-groups mean squares corresponds to interindividual (among replicates) error.

Definition of FGFR1 *polymorphisms*

Two SNPs (rs4647905:G>C and rs3213849:G>A), which represent >85% of the *FGFR1* gene haplotype variability found by Coussens and van Daal (2005), plus three other SNPs (rs2293971:G>A, rs2304000:G>C, and rs930828; T>C) situated nearby were genotyped in the 176 individuals of our sample using TaqMan assays. rs4647905:G>C and rs3213849:G>A are two haplotype-tag SNPs (htSNP) forming two distinct LD blocks, which include the rs2304000:G>C and rs2293971:G>A, as well as rs930828:T>C SNPs, respectively (Gómez-Valdés et al., 2013). Furthermore, our previous work showed that the two Mexican populations studied here (Gómez-Valdés et al., 2013), as European populations, present the two LD blocks previously found by Coussens and Daal (2005). Thus, two similar LD blocks are observed in both Totonaco and Mestizo populations, corroborating the suggestion that rs4647905 and rs3113849 are two haplotype-tag SNPs, as well as validating the haplotype tag SNPs associations performed here. Based on these and other previous results (see Introduction) only data from rs4647905:G>C and rs3213849G>A SNPs were used in the present genotype–phenotype relationship analysis described below. It is noteworthy that the allele frequencies in both populations are similar (Totonaco, rs4647905:G = 0.72 and s3213849; G = 0.70; Mexican Mestizo, rs4647905:G = 0.72 and s3213849:G = 0.64; Gómez-Valdés et al., 2013).

Quantification and characterization of morphological integration patterns

The recorded configurations of landmarks were subjected to GPA and the superimposed landmark coordinates were separated into two regions (i.e., the putative modules) (Fig. 1): the face and the vault, each one equally represented with 13 landmarks.

To account for common and local factors affecting head development we followed Mitteroecker and Bookstein (2007, 2008). The common factors were estimated as the dimensions of shape variation that are integrated among the face and the vault. The significance of the successive common factors was obtained after a permutation test

aimed to detect dimensions that differ significantly from a random distribution (Mitteroecker and Bookstein, 2008). The local factors defining the modular facial and neurocranial shape spaces were obtained using the residual scores of the multivariate regression of each block on the common factors. The resulting shape variables obtained in the different shape spaces were used to compute MANOVA tests aimed to detect between-samples, and among-genotypes differences, as well as its potential interactions.

After the computation of common and local factors, the pattern and magnitude of integration could be explored on four different shape spaces: (1) the full, (2) the integrated and the modular (3) facial and (4) head vault) shape spaces. First, analyses were made on the full shape space, representing the overlapped effects of integrated and modularized traits. Afterwards, MI between the face and the vault was assessed in the integrated shape space explained by the common factors, as well as in the modular shape spaces for the face and the vault, which complement the dimensions of the integrated shape space (Mitteroecker and Bookstein, 2008).

MI between the face and the vault in each of the shape spaces (full, integrated, and modular) was assessed using two-block partial least squares analysis (2B-PLS; Rohlf and Corti, 2000). 2B-PLS performs a singular value decomposition of the covariance matrix between two blocks of shape variables. Blocks of facial and vault landmarks were defined a priori (see Supporting Information Table 1), and the linear combinations of the original shape variables that provide the best mutual cross-prediction between these blocks of landmarks were computed. The amount of covariation was measured by the RV coefficient, which is a multivariate analog of the squared correlation (Klingenberg, 2009). To assess the statistical significance of the RV coefficient we performed permutation tests ($n = 10{,}000$) under the null hypothesis of complete independence between the two blocks of variables. To account for sexual and/or population differences the PLS analyses were based on the pooled within-population/sexes covariance matrix. The 2B-PLS function was run in R (R Development Core Team, http://www.R-project.org/), using the routine implemented by Sidney et al. (in press).

Our analyses were conducted using both rs4647905:G>C and rs3113849:G>A *FGFR1* htSNPs, but only those involving the first polymorphism showed significant results. In consequence, only the results regarding rs4647905:G>C will be reported. Differences in the integration patterns and magnitude among samples of individuals carrying different *FGFR1* polymorphisms were tested assembling different subsamples including (1) all individuals ($n = 176$), (2) only individuals carrying the CC genotype at the rs4647905:G>C site (derived homozygous state, $n = 17$), (3) only individuals carrying a GC genotype at the site (heterozygote state, $n = 63$), and (4) only individuals carrying the GG genotype at the site (ancestral homozygous state, $n = 96$). As stated above, separate PLS analyses were performed in the full shape space, the integrated shape space accounting for the common factors explaining the integrated shape aspects, and the residual modular shape spaces.

To test for differences among the covariance matrices across the four subsamples described above, we computed two-by-two matrix correlation tests between the corresponding pooled within-population and sex covariance matrices. For each analysis, a matrix permutation test against the null hypothesis of complete dissimilarity of the covariance matrices was performed by permuting landmarks and including the diagonals of the covariance matrices after 10,000 randomization rounds. Matrix correlations were computed for the full, the integrated, and the modular shape spaces using MorphoJ (Klingenberg, 2011).

Finally, we calculated the variance of the eigenvalues (EVs) (Wagner, 1984) as an estimator of overall integration between the face and vault, as well as to measure and compare the magnitude of integration within the face and the vault across different subsamples on the different shape spaces (full, integrated and modular). High EV is characteristic of highly integrated phenotypic units, whereas low EV is typical of phenotypes with low integration (Wagner, 1984; Young, 2006). The variance/covariance matrices of the Procrustes coordinates of the left face ($K = 8$, where K is the number of landmarks), the left vault ($K = 8$), and the whole head (face+vault, $K = 16$) were calculated for each subsample separately. Only the left side was used to avoid data matrices containing zero elements, which are frequent on landmark configurations with object symmetry. From each variance-covariance matrix, we computed the EVs and obtained ranges of EV integration values by resampling each dataset with replacement for 1,000 iterations. To compare the integration measures across groups and remove variation in the index caused by the magnitude of the overall variance we standardized the EV scores by the total shape variance within the entire sample group following Young (2006). Resampled datasets were fixed to represent the lowest sample size (CC = 17 individuals) to avoid bias on the computation of EV ranges due to the lower sample size of such subsample. These procedures were calculated using the PopTools plug-in for Excel version 3.2 (http://www.poptools.org).

FGFR1 *molecular simulations*

As a final complementary analysis, we explored the putative splicing events caused by the studied mutations, as well as the concomitant changes on protein structure. To do so, and considering that the rs4647905:G>C polymorphism is located in an intronic region of a gene known for its high protein variation due to alternative splicing, we sought within the sequence that flanks it the possible alternative splice and binder sites using the Alternative Splicing and Transcript Diversity Databases (http://www.ebi.ac.uk/asd/ index.html).

RESULTS

Repeatability analysis

Mean landmark deviation was 0.0067 (min. = 0.0019, max. = 0.0177) and 0.0019 (min. = 0.0009, max. = 0.0059) Procrustes distance units for the interindividual and the inter-replicate (within individual) errors, respectively. The greatest repeatability errors were detected on the landmarks vertex, left euryon, and right euryon, whereas the lower errors were measured on left orbital, right orbital, and left endocanthion. The ANOVA results showed that the mean interindividual RMSE is 0.0101 and 0.002 for the inter-replicate comparison. For all landmarks, the interindividual differences are well above the inter-replicate error and, in most cases, this difference is

of one order of magnitude. Considering the relatively large size of the heads studied here, and that the inter-replicate error is clearly lower than the interindividual differences, the margins of error were considered acceptable.

Morphological integration patterns

Analyses considering variations at the rs3113849:G>A *FGFR1* htSNP, and the joint two tag-SNPs showed no differences in the magnitude and/or patterns of integration across the different allelic subsamples. However, some potentially interesting variations were found regarding the rs4647905:G>C SNP. After the computation of common and local factors, the pattern and magnitude of integration was explored in the four shape spaces (full, integrated, and modular × 2) that span the complex nature of the human head.

Supporting Information Table 2 presents the MANOVA results depicting shape differences among the studied groups. Native-Admixed differences are observable on all the shape spaces considered here, whereas there are no shape differences among genotypes or population-genotype interactions. Thus, the question arises if alleles at the rs4647905:G>C position alter the normal pattern of MI, rather than generating overall shape changes. The covariation pattern between the vault and the face was used to evaluate this hypothesis. Partial least squares analysis provided descriptions of the vault and the face configurations, as well as estimations of the covariation between these two blocks.

TABLE 1. Results of the PLS analyses performed on the full shape space

	RV coefficient	*P*	Expl. Covar. PLS1	Corr PLS1	*P*
All groups	0.09	<0.0001	33.0	0.519	<0.0001
CC	0.51	0.0056	66.2	0.799	0.1013
GC	0.20	0.0013	40.0	0.667	0.0003
GG	0.14	0.0004	39.1	0.590	0.0001

For each subsample, we provide the RV coefficient of overall integration between the face and the neurocranium and the associated *P* value; the percentage of total covariation explained by the PLS1 axes; the correlation score between facial and neurocranial PLS1 scores and the associated *P* value.

When the full shape space is analyzed using PLS, results show that the first pair of PLS axes (PLS1) explains 33.0% of the total covariance and that the overall strength of the association between face and vault is low (RV = 0.09), but statistically significant (Table 1). Individuals carrying different alleles at the rs4647905:G>C site completely overlap, showing a common pattern of integration and suggesting the nonrejection of the first null hypothesis of equal patterns of integration among genotypes (Fig. 2). Covariation among the face and the vault is mainly shaped by an anterior–posterior expansion of the mandible, combined with an anterior expansion of the nose, and a lateral expansion of the endocanthion and exocanthion (medial and lateral borders of the eye, respectively). These facial changes (Fig. 2, left wireframes) are associated with more elongated and narrower vaults. To evaluate if the rs4647905:G>C polymorphism is associated with changes in the magnitude of MI, we obtained RV coefficients from PLS analyses performed separately for each of the different subsamples of individuals carrying different genotypes. In comparison with the pooled sample, individuals carrying the CC derived homozygous condition show a stronger and significant integration (RV = 0.51, 66.2% of explained covariance) between the face and the vault. The PLS performed on the GC and GG subsamples provided lower levels of integration (RV = 0.20 and 0.14, respectively). Thus, even though the pattern by which the face and the vault covary is similar in the different genotype subsamples (Fig. 2), individuals carrying the CC homozygous genotype present a higher

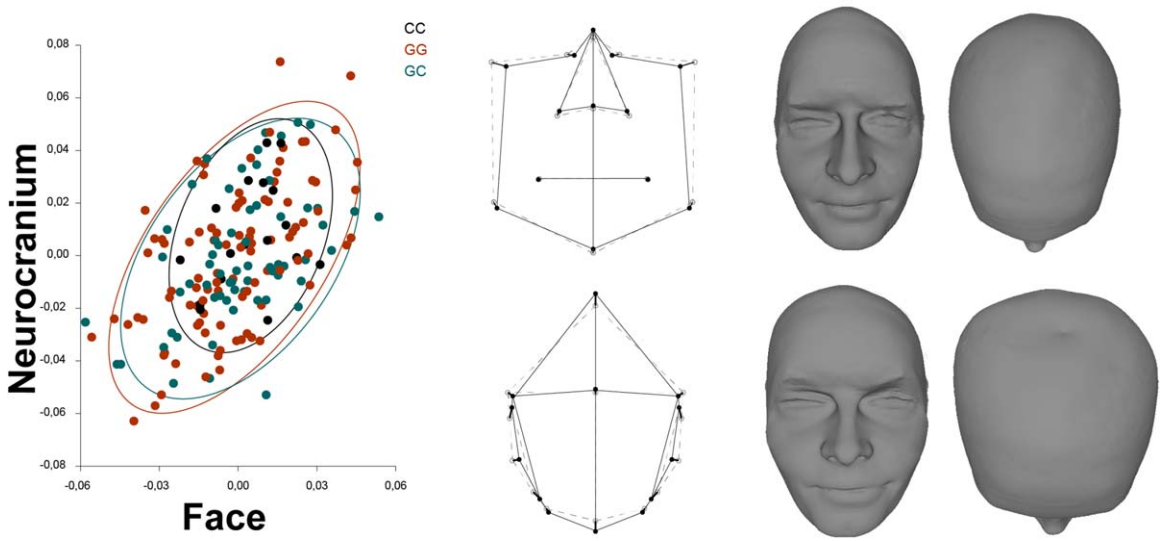

Fig. 2. Scatterplots of PLS1 scores of the face and neurocranium computed on the full shape space. 90% confidence ellipses are shown for the CC, GC, and GG subsamples. Wireframes depict the facial (top) and neurocranium (bottom) shape changes in frontal and superior view, respectively associated to displacements across the first PLS from the consensus. Surface morphs representing the shape changes in frontal and superior view associated to increasing (top) and decreasing (bottom) scores from the consensus are presented on the right side. [Color figure can be viewed in the online issue, which is available at wileyonlinelibrary.com.]

intensity of MI between the face and the vault. This supports the rejection of the second null hypothesis of no differences on the magnitude of MI across variants of the *FGFR1* gene.

Regarding the levels of covariation in the integrated shape space, seven significant common factors were extracted from the whole sample, three from the CC and GC subsamples, and six from the GG subsample. When the first two common factors of the whole sample (together explaining 47% of the total covariation) are plotted (Supporting Information Fig. 2), it is evident that there are no differences in the pattern of integration among the different subsamples. However, and as observed in Table 2, the first common factor of the rs4647905:G>C–CC sample explains higher variance and covariance than the first common factor of the remaining subsamples (GC and GG) or the full sample. In sum, our results indicate that the integrated space is characterized by stronger integration in the CC subsample, whereas there are no differences among subsamples in the pattern of integration. As a whole, results of the analyses performed on the integrated space suggest nonrejection of the first null-hypothesis (equality on integration patterns) and rejection of the second specific null hypothesis indicating significant differences in the magnitude of MI among *FGFR1* polymorphisms.

To further explore the role of the rs4647905:G>C allelic variant we replicated the PLS analyses considering the modular shape spaces, which were obtained from the residuals of the multivariate regression of each block's shape coordinates on the significant common factors of each subsample. Results are presented in Table 3, and they replicate the results obtained in the full-shape space analyses: carriers of the homozygous derived *C* allele tend to present higher levels of covariance ($RV_{CC} = 0.51$, versus $RV_{All\ individuals}$ 0.19, $RV_{GC} = 0.19$, and $RV_{GG} = 0.22$). Again, the pattern of integration does not differ among subsamples (Fig. 3). In general, these results indicate nonrejection of the first null hypothesis and rejection of the second one.

Covariation patterns in the modular shape spaces slightly differ from the full-shape space analysis, mainly because facial changes involve a lateral expansion of the mouth, a superior displacement of the tip of the nose, in combination with a posterior–superior displacement of euryon (Fig. 3, left and right wireframes). When compared to the shape changes observed on the full shape-space (Fig. 2), the pattern of covariation depicted on the modular space is restricted to more localized changes in the mouth, the nose, and the lateral walls of the head.

TABLE 2. Results corresponding to the first common factors (cf1) of the total sample in the three subsamples analyzed

	Cov cf1	Corr cf1	Expl. Var. Cf1	Expl. Covar. Cf1	*P*
All groups	3.82	0.770	21.1	32.7	0.001
CC	7.01	0.867	30.8	35.0	0.002
GC	3.52	0.804	20.1	28.3	0.001
GG	4.00	0.775	21.8	30.8	0.001

Covariance (*n* units of squared Procrustes distances ×104) and correlation among the first singular scores of face and neurocranium are presented, along with the percentage of the variance and covariance explained by the common factors, and the *P* value of each common factor.

TABLE 3. Results of the PLS analyses performed on the modular shape space

	RV coefficient	*P*	Expl. Covar.	Corr PLS1	*P*
All groups	0.19	<0.0001	48.0	0.750	<0.0001
CC	0.51	0.005	45.0	0.870	0.0333
GC	0.19	0.0071	30.2	0.724	<0.0001
GG	0.22	<0.0001	41.9	0.672	<0.0001

For each subsample, we provide the RV coefficient of overall integration between the face and the neurocranium and the associated *P* value; the percentage of total covariation explained by the PLS1 axes; the correlation score between facial and neurocranial PLS1 scores and the associated *P* value.

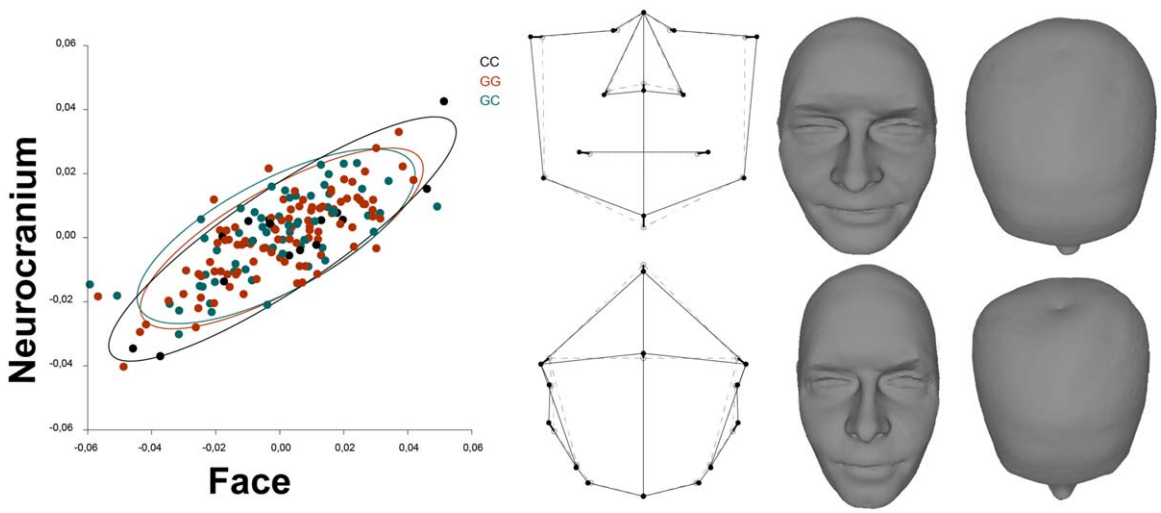

Fig. 3. Scatterplots of PLS1 scores of the face and neurocranium computed on the modular shape space. 90% confidence ellipses are shown for the CC, GC, and GG subsamples. Wireframes depict the facial (top) and neurocranium (bottom) shape changes in frontal and superior view, respectively associated to displacements across the first PLS from the consensus. Surface morphs representing the shape changes in frontal and superior view associated to increasing (top) and decreasing (bottom) scores from the consensus are presented on the right side. [Color figure can be viewed in the online issue, which is available at wileyonlinelibrary.com.]

TABLE 4. Matrix correlation results

Whole	All groups	CC	GC	GG
All groups	–	0.816	0.939	0.979
CC	0.620	–	0.706	0.758
GC	0.925	0.518	–	0.866
GG	0.958	0.543	0.812	–
Face	All groups	CC	GC	GG
All groups	–	0.837	0.947	0.946
CC	0.589	–	0.789	0.754
GC	0.905	0.534	–	0.842
GG	0.948	0.560	0.810	–
Neurocranium	All groups	CC	GC	GG
All groups	–	0.892	0.955	0.986
CC	0.662	–	0.811	0.859
GC	0.788	0.667	–	0.901
GG	0.927	0.593	0.736	–

Figures above and below the diagonal correspond to Matrix correlation values computed on the full and the modular shape space, respectively. All correlations are significant at $P < 0.0001$.

The PLS results were further corroborated by the matrix correlation tests, that confirm that all subsamples (CC, GC, GG) present similar covariation patterns between the face and the vault. The matrix correlation values are presented in Table 4, and they show that, even if subsamples involving the homozygous CC variant at the rs4647905:G>C position slightly differ from the remaining subsets, all the two-by-two comparisons yielded high and significant matrix correlation values, thus demonstrating an overall similarity on integration patterns across different genetic variants of the *FGFR1* system. When matrix correlation tests are computed on the modular shape space, there is a general decrease on the correlation values involving the CC subsamples (average correlation on the full space = 0.84 vs. average correlation on the modular space = 0.67), thus suggesting a slight difference in the pattern of integration not evidenced by the PLS analyses.

The variance of the EVs was used to further estimate the overall strength of integration within and between the face and neurocranium on the different subsamples and shape spaces. Results on the full shape space show that the CC subsample displays greater between and within-block integration. Particularly, there is a significantly higher integration of the whole head in the CC subsample. The EV analyses computed on the shape space spanned by the common factors (i.e., the integrated shape space) further corroborate this trend of greater integration in the CC subsample, whereas the tendency vanishes on the modular space (Fig. 4). In this regard, the most striking result is that the observed EV value of the common factors of the CC subsample falls well above the values of the remaining subsamples of common factors.

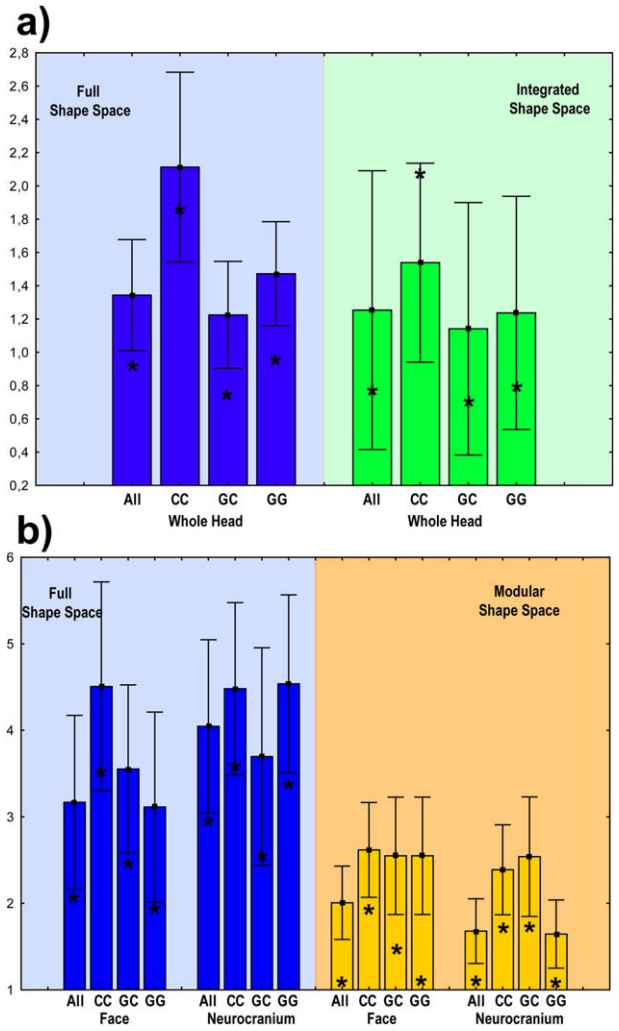

Fig. 4. Comparison of the magnitude of morphological integration within and between the face and the neurocranium across subsets representing different genetic variants of the FGFR1 gene. Bar graphs with standard deviation error bars comparing the distribution of the integration index (EV, eigenvalue variance standardized by group variance $\times 10^5$) between the face and the neurocranium (whole head) in the full (blue bars) and the integrated (green bars) spaces (a); and within the face and within the neurocranium in the full (blue bars) and modular (orange bars) spaces (b). Black asterisks denote the observed eigenvalue variance for each computation. [Color figure can be viewed in the online issue, which is available at wileyonlinelibrary.com.]

FGFR1 *molecular simulations*

When the rs4647905:G>C polymorphism is explored in relation to their effect on binding sites and protein structure, results indicate that the simulation of an amino-acid change from G to C results in a specific binding site for the splicing factor SRp40, whereas the preservation of a G nucleotide in this position generates a hnRNPH, which are known promoter and inhibitor splicing factors, respectively.

Additionally, to investigate the feasibility of a possible splicing site in this region, we looked for AG sequences, which are termination indicators of introns and alternative start codons in humans. We found a viable sequence nearby the rs4647905:G>C mutation, which could lead to the insertion of nucleotides in the adjacent exon without any change in the reading frame. We also looked for putative changes linked to this amino acid inclusion in the exon adjacent to the mutation in the secondary and tertiary structure of the alternative protein (Lambert et al., 2002), as well as to the behavior of transmembrane structures (Juretic et al., 2002). Our analyses indicate that an aminoacid insertion results in a viable protein containing different secondary and tertiary structures, along with a probable new transmembrane structure.

DISCUSSION

Our analyses reveal that there are no shape differences among genotypes or population–genotype interactions (see Supporting Information Table 2), but significant among-genotype differences regarding the pattern and magnitude of MI. Even though we detected that the FGFR1 mutations studied here are mainly related to the length of the head vault (individuals carrying the derived alleles in both sites exhibit head lengths increased in the antero-posterior axis, especially among the admixed sample, Gómez-Valdés et al., 2013), the current more refined shape analysis did not show significant shape differences among genotypes. The lack of shape differentiation between the three FGFR1gene variants can have several origins. First, the mutation might not have a strong detectable developmental effect. Thus, it is possible that these polymorphisms only affect some specific, localized aspects of head shape, and this global analysis involving three-dimensional landmark configurations (rather than measurements) indicates a weak or null signal of developmental shifts deriving on adult shape variations.

Second, there might be patterns of epistasis that the data collected do not explain, as suggested by Hallgrímsson and Lieberman (2008) as the "epigenetic funnel." This definition focuses on the idea that in many developmental systems developmental processes can be identified that are particularly important determinants of some type of phenotypic variation. Such processes may be influenced by many developmental-genetic pathways and often by a vast number of potential mutations. In general, a vast array of genetic variation is "funneled" to a smaller set of pathways, which in turn influence a smaller set of developmental processes (Hallgrimsson and Lieberman, 2008; Hallgrimsson et al., 2007, 2009). To what extent the FGFR1 mutations studied here are funneled in this way is still unknown, but the possibility that this mechanism is operating to blur some shape-difference generating process should not be disregarded. An additional, nonexclusive hypothesis is that there might be other correlated genes that differ between the samples but which have not been analyzed.

Regardless the lack of shape differences among the genotypes studied, the analyses performed here suggest a role of the homozygous state of the mutation from G to C at the rs4647905:G>C position as an enhancer of MI intensity. This aminoacid change, however, does not affect the covariation pattern of the two subsamples (Totonaco Native American and Mexican Mestizo populations) analyzed here. Results from the PLS analyses computed on the full, integrated, and modular shape spaces independently confirmed that the pattern of integration among the face and the neurocranium is similar on the subsamples of CC, GC and GG individuals (Figs. 2 and 3), indicating nonrejection of the first null-hypothesis; whereas the magnitude of the integration is higher on carriers of the CC genotype, particularly when the integrated space spanned by the common factors is considered (rejection of the second null hypothesis) (Tables (1–4) and Fig. 4).

///////Overall, our results complement previous findings on developmental biology research (Bertrand et al., 2011; Martínez-Abadías et al., 2012, 2013), providing further evidence of the general role of the FGF/FGFR signaling pathway in head development. We have shown that in two human populations certain variants of the *FGFR1* gene correspond to different head shapes (González-Valdés, 2012) and that these *FGFR1* variants can also be associated with different magnitudes of integration within the head.

Morphological integration patterns

Hallgrímsson et al. (2007) proposed that the covariation structure observed in adult phenotypes is the final outcome of a series of successive covariance-generating developmental processes that leave (and superimpose) its traces since the early phases of embryonic development. Accordingly, each covariance-generating process will blur or obscure the effects of the others on the overall covariance structure (Hallgrímsson et al., 2009). Thus, MI patterns in the vertebrate skull arise as a superposition of covariation patterns determined at different, consecutive, or overlapping developmental processes that modulate the relationships among different structures as the individual develops (Hallgrímsson et al., 2007). Moreover, the simultaneous action of common factors promoting pervasive integration at the global scale, overlapping with local factors generating modular patterns contribute to the spectrum of adult variation and covariation patterns (Mitteroecker and Bookstein, 2007, 2008).

Evidence from previous works supports the integrated but yet modular structure of the head, at least at the skull level. For instance, in the human skull, the general pattern and magnitude of genetic and phenotypic integration was suggested to be pervasive (Martínez-Abadías et al., 2012) and conserved across different, worldwide dispersed populations (González-José et al., 2004). Other works detected varying levels of integration among parts on the primate skull (Ackermann, 2005; Cheverud, 1995; Lieberman et al., 2000, 2002; Marroig and Cheverud, 2001; Strait, 2001), and on human samples characterized by osseous malformations (Richtsmeier and Deleon, 2009), or cultural deformation practices (Martínez-Abadías et al., 2009), and differences in integration and modular patterns within and between species have been highlighted. Finally, knowledge of the developmental processes (Enlow, 1996; Helms et al., 2005; Lieberman, 2000; Sperber, 2001; Tapadia et al., 2005) and functional demands (González-José et al., 2005; Paschetta et al., 2010) underlying the different regions of the human skull further supports the existence of modules.

In consequence, studying disruptions in the pattern and magnitude of MI in the full, the integrated and the modular shape subspaces can be useful to disentangle the genotype–phenotype map underlying size and shape variation of the human head. Here, we have analyzed how mutations in a specific gene (*FGFR1*) expressed in a signaling pathway relevant for head development (i.e., *FGF*/*FGFR*) can potentially affect the pattern and intensity of covariation between the face and the vault. Note that, even when more research on covariation patterns of soft-tissue structures are needed, preliminary comparisons with previous studies evaluating the effects of *FGFR* genes made on hard, bony structures is relatively accurate given the results obtained in a previous, specific analysis focused on the relationship of facial soft tissues to dry skulls that obtained significant correlations between soft-tissue depths of the face and craniometric dimensions (Simpson and Henneberg, 2002).

To the best of our knowledge, this is the first test of the effect of specific mutations of a candidate gene on

integration patterns of a human normal spectrum of variation. The main result of our study, independently confirmed by three different approaches of quantification and characterization of MI, is that individuals carrying a homozygous derived state on a specific intronic site (i.e., the CC genotype) tend to show more tightly integrated faces and vault. Noteworthy, the same tendency was observed independently in both Natives and Mexican Mestizos, indicating that any eventual difference in the genome background of these two groups has little relevance in altering the connection between the CC genotype and MI.

The pleiotropic effect of variants of major genes such as *FGFR1* (Table 1, Fig. 4) is corroborated by the stronger level of integration among the face and the vault observed on the space delimitated by the common factors (i.e., the portion of the shape space that occupies the morphological aspects explained by covariation among both structures) by carriers of the C allele at the rs4647905:G>C site. Differences on the pattern and magnitude of integration among rs4647905:G>C variants computed on the modular subspace are less evident. Differences in the patterns of MI are intuitively expected in the neurocranium simply because the sutures of clinical interest occurring in individuals with craniofacial dysmorphologies are located there. However, previous research (Bachler et al., 2001; Martínez-Abadías et al., 2010; Szabo-Rogers et al., 2008; Wilke et al., 1997) indicates that FGF/FGFR is strongly expressed in the face and, in craniosynostotic syndromes, it causes severe facial hypoplasia.

FGFR1 *molecular simulations*

Considering the above results, it is valid to speculate about the putative effects that such mutation can induce on the structural properties of the *FGFR1* gene product. The *FGFR1* gene is one of the most illustrative examples of nonconservative splicing. Previous studies have demonstrated that *FGFR1* alternative splicing modifies both extracellular and intracellular domains of this receptor, resulting in forms that vary in their affinity and ligand-binding specificity for fibroblast growth factor (Bruno et al., 2004; Coussens and Daal, 2005). mRNA alternative splicing promotes the increase of the gene coding capacity, allowing the synthesis of several structurally and functionally distinct proteins (Cáceres and Kornblihtt, 2002). Both alternative and constitutive pre-mRNA splicing require the presence of the 3' and 5' splice sites, branch site, as well as additional positive (enhancer) and negative (silencer) regulatory sequence elements. The complex connection between several different categories of the *trans*-acting factors that recognize these enhancer and/or silencer *cis*-acting sequence elements (which can be either exonic or intronic) directly modulates the formation of the spliceosome, regulating the pre-mRNA splicing (Cáceres and Kornblihtt, 2002). However, intronic splicing enhancer/silencer elements are less well known, and consequently the examples are scarce. Here, we speculate that the presence of the rs4647905 C allele results in an intronic specific binding site for a SRp40 element, a known enhancer-splicing factor. Additionally, other modifications in the adjacent exon may occur due to the G>C mutation. Interestingly, preliminary results of the 1,000 Genomes Project (Available at: http://browser.1000genomes.org/Homo_sapiens/Variation/Mappings?db=core;r=8:38272042–38273042;v=rs4647905;vdb=variation;vf=3547741) also suggest that there are transcript variations containing the rs4647905 C allele.

Our findings suggest that the *FGFR1* rs4647905:G>C SNP, although located in an intronic region, can be functional, being directly responsible for global, pervasive changes on the magnitude of skull integration. However, caution is needed regarding this suggestion, since our analyses were developed *in silico* only. Additional functional studies may reveal whether the above-mentioned SNP is itself causal or if it is in linkage disequilibrium with unknown, true causal variants. In this regard, note that we previously demonstrated that rs4647905:G>C is in a linkage disequilibrium block in the Mestizo and Native American populations (Gómez-Valdés et al., 2013). The tissue specificity of the *FGFR1* splicing is another factor that should be investigated through functional approaches to validate the hypothesis presented here.

CONCLUSIONS

Our results provide additional evidence about integration-generating mechanisms operating in the evolution and development of the human head. Specifically, we have tested for differences in integration patterns and magnitude rather than on absolute shape differences, as was previously explored in Coussens and Daal (2012) and Gómez-Valdés et al. (2013). We have done so using a novel and powerful method that specifically enables the dissociation of the fraction of variation due to common factors such as pleiotropic genetic effects, from that of local factors such as tissue-specific signaling (Mitteroecker and Bookstein, 2007). Also, our study contributes to the necessary verification of inferences made using mouse models in humans (e.g., Martínez-Abadías et al., 2011, 2012). Finally, our results are interpreted taking into account splicing events, which are important and ubiquitous in the evolution of *FGFR1*. Future investigations on the effect of specific mutations in genes participating in signaling and regulatory complexes will benefit from analyses focusing on functional structural properties of gene products and by more refined approaches to morphology, considering not only pure size and shape changes but also patterns of integration, modularity, canalization, and developmental stability of complex phenotypes.

ACKNOWLEDGMENTS

The authors express our gratitude to Samuel Canizales, Paola Everardo and Rodrígo Barquera for their support during laboratory activities and Gastón Macín Pérez for helping during the geometric morphometric data collection. Ascención Ortíz is thanked for developing the cephalostate device used to fix the head during the digitizing process. Carina Ambrosio is also acknowledged by its collaboration during the elaboration of this article. The authors declare no conflict of interest.

LITERATURE CITED

Ackermann RR. 2005. Ontogenetic integration in the hominoid face. J Hum Evol 48:175–197.

Bachler M, Neubüser A. 2001. Expression of members of the Fgf family and their receptors during midfacial development. Mech Dev 100:313–316.

Bastir M, Rosas A, Stringer C, Cuétara JM, Kruszynski R, Weber GW, Ross CF, Ravosa MJ. 2010. Effects of brain and facial size on basicranial form in human and primate evolution. J Hum Evol 58:424–431.

Bertrand S, Camasses A, Somorjai I, Belgacem MR, Chabrol O, Escande M-L, Pontarotti P, Escriva H. 2011. Amphioxus FGF signaling predicts the acquisition of vertebrate morphological traits. Proc Natl Acad Sci USA 108:9160–9165.

Bruno IG, Jin W, Cote GJ. 2004. Correction of aberrant *FGFR1* alternative RNA splicing through targeting of intronic regulatory elements. Hum Mol Gen 13:2409–2420.

Cáceres JF, Kornblihtt AR. 2002. Alternative splicing: multiple control mechanisms and involvement in human disease. Trends Genet 18:186–193.

Cheverud JM. 1982. Phenotypic, genetic, and environmental integration in the cranium. Evol 36:499–516.

Cheverud JM. 1984. Quantitative genetics and developmental constraints on evolution by selection. J Theor Biol 110:155–171.

Cheverud JM. 1995. Morphological integration in the saddle-back tamarin (Saguinus fuscicollis) cranium. Am Nat 145:63–89.

Cheverud JM. 1996. Developmental integration and the evolution of pleiotropy. Am Zool 36:44–50.

Cohen MJ, MacLean R. 2000. Craniosynostosis: diagnosis, evaluation, and management. Oxford: Oxford University.

Coussens AK, Daal A. 2005. Linkage disequilibrium analysis identifies an FGFR1 haplotype-tag SNP associated with normal variation in craniofacial shape. Genomics 85:563–573.

Cunningham ML, Seto ML, Ratisoontorn C, Heike CL, Hing AV. 2007. Syndromic craniosynostosis: from history to hydrogen bonds. Orthod Craniofac Res 10:67–81.

Dorey K, Amaya E. 2010. FGF signaling: diverse roles during early vertebrate embryogenesis. Development 137:3731–3742.

Enlow D, Hans M. 1996. Essentials of Facial Growth. New York: Saunders Company.

Esteve-Altava B, Marugán-Lobón J, Botella H, Bastir M, Rasskin-Gutman D. 2013. Grist for Riedl's Mill: a network model perspective on the integration and modularity of the human skull. J Exp Zool B Mol Dev Evol doi: 10.1002/jez.b.22524 [Epub ahead of print].

Gómez Valdés J, Hünemeier T, Contini V, Acuña-Alonzo V, Macin G, Ballesteros-Romero M, Corral P, Ruiz-Linares A, Sanchez-Mejorada G, Canizales-Quinteros S, Martinez-Abadias N, Salzano FM, Gonzalez-José R, Bortolini MC. 2013. Fibroblast growth factor receptor 1 variants and craniofacial variation in Amerindians and related populations. Am J Hum Biol 25:12–19.

González-José R, Ramírez-Rozzi F, Sardi M, Martínez-Abadías N, Hernández M, Pucciarelli HM. 2005. A functional-cranial approach to the influence of economic strategy on skull morphology. Am J Phys Anthropol 128:757–771.

González-José R, Van der Molen S, González-Pérez E, Hernández M. 2004. Patterns of phenotypic covariation and correlation in modern humans as viewed from morphological integration. Am J Phys Anthropol 123: 69–77.

Goswami A. 2006. Cranial modularity shifts during mammalian evolution. Am Nat 168:270–280.

Griswold CK. 2006. Pleiotropic mutation, modularity and evolvability. Evol Dev 8:81–93.

Groth C, Lardelli M. 2002. The structure and function of vertebrate fibroblast growth factor receptor 1. Int J Dev Biol 46:393–400.

Hajihosseini MK, Duarte R, Pegrum J, Donjacour A, Lana-Elola E, Rice DP, Sharpe J, Dickson C. 2009. Evidence that Fgf10 contributes to the skeletal and visceral defects of an Apert syndrome mouse model. Dev Dyn 238:376–385.

Hallgrímsson B, Lieberman DE. 2008. Mouse models and the evolutionary developmental biology of the skull. Integr Comp Biol 48:373–384.

Hallgrímsson B, H, Young NM, Rolian C, Parsons TE, Boughner JC, Marcucio RS. 2009. Deciphering the Palimpsest: studying the relationship between morphological integration and phenotypic covariation. Evol Biol 36:355–376.

Hallgrímsson B, Lieberman DE, Liu W, Ford-Hutchinson AF, Jirik FR. 2007. Epigenetic interactions and the structure of phenotypic variation in the cranium. Evol Dev 9:76–91.

Hansen TF, Houle D. 2008. Measuring and comparing evolvability and constraint in multivariate characters. J Evol Biol 21:1201–1219.

Helms JA, Cordero D, Tapadia MD. 2005. New insights into craniofacial morphogenesis. Development 132:851–861.

Jiang X, Iseki S, Maxson RE, Sucoy HM, Morriss-Kay GM. 2002. Tissue origins and interactions in the mammalian skull vault. Dev Biol 241: 106–116.

Jin W, Huang ES, Bi W, Cote GJ. 1999. Redundant intronic repressors function to inhibit fibroblast growth factor receptor-1 alpha-exon recognition in glioblastoma cells. J Biol Chem 274:28035–28041.

Juretic D, Zoranić L, Zucić D. 2002. Basic charge clusters and predictions of membrane protein topology. J Chem Inf Comput Sci 42:620–632.

Klingenberg CP. 2008. Morphological integration and developmental modularity. Annu Rev Ecol Syst 39:115–132.

Klingenberg CP. 2009. Morphometric integration and modularity in configurations of landmarks: tools for evaluating a priori hypotheses. Evol Dev 11:405–421.

Klingenberg CP. 2011. MorphoJ: an integrated software package for geometric morphometrics. Mol Ecol Resour 11:353–357.

Lambert C, Leonard N, De Bolle X, Depiereux E. 2002. ESyPred3D: prediction of proteins 3D structure. Bioinformatics 18:1250–1256.

Lieberman DE, McBratney BM, Krovitz GE. 2002. The evolution and development of cranial form in *Homo sapiens*. Proc Natl Acad Sci USA 99:1134–1139.

Lieberman DE, Ross C, Ravosa MJ. 2000. The primate cranial base: ontogeny, function, and integration. Yearb Phys Anthropol 43:117–169.

Lieberman DE. 2011. The evolution of human head. Cambridge: The Belknap Press of Harvard University.

Marroig G, Cheverud JM. 2001. A comparison of phenotypic variation and covariation patterns and the role of phylogeny, ecology, and ontogeny during cranial evolution of new world monkeys. Evol 55:2576–2600.

Martínez-Abadías N, Esparza M, Sjøvold T, González-José R, Santos M, Hernández M, Klingenberg CP. 2012. Pervasive genetic integration directs the evolution of human skull shape. Evol 66:10–23.

Martínez-Abadías N, Heuzé Y, Wang Y, Jabs EW, Aldridge K, Richtsmeier JT. 2011. FGF/FGFR signaling coordinates skull development by modulating magnitude of morphological integration: evidence from Apert syndrome mouse models. PLoS ONE 6:e26425.

Martínez-Abadías,N, P Mitteroecker, TE Parsons, M Esparza, T Sjøvold, C Rolian, JT Richtsmeier, B Hallgrímsson. 2012. The developmental basis of quantitative craniofacial variation in humans and mice. Evol Biol 39: 554–567.

Martínez-Abadías N, Motch SM, Pankratz TL, Wang Y, Aldridge K, Jabs EW, Richtsmeier JT. 2013. Tissue-specific responses to aberrant FGF Signaling in complex head phenotypes. Dev Dyn 242:80–94.

Martínez-Abadías N, Paschetta C, Azevedo S, Esparza M, González-José R. 2009. Developmental and genetic constraints on neurocranial globularity: insights from analyses of deformed skulls and quantitative genetics. Evol Biol 36:37–56.

Martínez-Abadías N, Percival C, Aldridge K, Hill CA, Ryan T, Sirivunnabood S, Wang Y, Jabs EW, Richtsmeier JT. 2010. Beyond the closed suture in apert syndrome mouse models: evidence of primary effects of FGFR2 signaling on facial shape at birth. Dev Dyn 239:3058–3071.

Mitteroecker P, Bookstein FL. 2007. The conceptual and statistical relationship between modularity and morphological integration. Syst Biol 56:818–836.

Mitteroecker P, Bookstein FL. 2008. The evolutionary role of modularity and integration in the hominoid cranium. Evol 62:943–958.

Moss M, Young R. 1960. A functional approach to craniology. Am J Phys Anthropol 18:281–291.

Nie X, Luukko K, Kettunen P. 2006. FGF signaling in craniofacial development and developmental disorders. Oral Dis 12:102–111.

Olson EC, Miller RL. 1958. Morphological integration. Chicago: University of Chicago.

Ornitz DM, Itoh N. 2001. Fibroblast growth factors. Genome Biol 2:1–12.

Paschetta C, de Azevedo S, Castillo L, Martínez-Abadías N, Hernández M, Lieberman DE, González-José R. 2010. The influence of masticatory loading on craniofacial morphology: a test case across technological transitions in the Ohio Valley. Am J Phys Anthropol 141:97–314.

Porto A, Oliveira FB, Shirai LT, Conto V, Marroig G. 2008. The evolution of modularity in the mammalian skull I: morphological integration patterns and magnitudes. Evol Biol 36:118–135.

Raff RA, Sly BJ. 2000. Modularity and dissociation in the evolution of gene expression territories in development. Evol Dev 2:102–113.

Raff RA. 1996. The shape of life: genes, development, and the evolution of animal form. Chicago: University Chicago Press.

Richtsmeier JT, Deleon VB. 2009. Morphological integration of the skull in craniofacial anomalies. Orthod Craniofac Res 12:149–158.

Robin NH, Falk MJ, Haldeman-Englert CR. FGFR-Related Craniosynostosis Syndromes. 1998 Oct 20 [Updated 2011 Jun 7]. In: Pagon RA, Adam MP, Bird TD, et al., editors. GeneReviews^{TM} [Internet]. Seattle (WA): University of Washington, Seattle; 1993–2013. Available from: http://www.ncbi.nlm.nih.gov/books/NBK1455/.

Rohlf FJ, Corti M. 2000. The use of two-block partial least-squares to study covariation in shape. Syst Biol 49:740–753.

Rohlf FJ, Slice DE. 1990. Extensions of the procrustes method for the optimal superimposition of landmarks. Syst Zool 39:40–59.

Schluter D. 1996. Adaptive radiation along genetic lines of least resistance. Evol 50:1766–1774.

Simpson E, Henneberg M. 2002. Variation in soft-tissue thicknesses on the human face and their relation to craniometric dimensions. Am J Phys Anthropol 118:121–133.

Singleton M. 2002 Patterns of cranial shape variation in the Papionini (Primates: Cercopithecinae). J Hum Evol 42:547–578.

Sperber GH. 2001. Craniofacial development. Hamilton: BC Decker.

Strait DS. 2001. Integration, phylogeny, and the hominid cranial base. Am J Phys Anthropol 114:273–297.

Stringer C. 2002. Modern human origins: progress and prospects. Phil Trans R Soc Lond B 357:563–579.

Sydney NV, Machado FA, Hingst-Zaher E. Timing of ontogenetic changes of two cranial regions in Sotalia guianensis (Delphinidae). Mamm Biol 77:397–403.

Szabo-Rogers HL, Geetha-Loganathan P, Nimmagadda S, Fu KK, Richman JM. 2008. FGF signals from the nasal pit are necessary for normal facial morphogenesis. Dev Biol 318:289–302.

Szabo-Rogers HL, Smithers LE, Yakob W, Liu KJ. 2010. New directions in craniofacial morphogenesis. Dev Biol 341:84–94.

Tapadia MD, Cordero D, Helms JA. 2005. It's all in your head: new insights into craniofacial development and deformation. J Anat 207: 461–477.

Trinkaus E. 2003. Proc Natl Acad Sci USA 100:8142–8145.

Wagner GP, Altenberg L. 1996. Complex adaptations and the evolution of evolvability. Evol 50:967–976.

Wagner GP. 1984. On the eigenvalue distribution of genetic and phenotypic dispersion matrices: evidence for a non-random origin of quantitative genetic variation. J Math Biol 21:77–95.

Wilke TA, Gubbels S, Schwartz J, Richman JM. 1997. Expression of fibroblast growth factor receptors (FGFR1, FGFR2, FGFR3) in the developing head and face. Dev Dyn 210:41–52.

Willmore KE, Leamy L, Hallgrimsson B. 2006. Effects of developmental and functional interactions on mouse cranial variability through late ontogeny. Evol Dev 567:550–567.

Willmore KE, Young NM, Richtsmeier JT. 2007. Phenotypic variability: its components, measurement and underlying developmental processes. Evol Biol 34:99–120.

Young NM. 2006. Function, ontogeny and canalization of shape variance in the primate scapula. J Anat 209:623–636.

Zelditch ML. 1988. Ontogenetic variation in patterns of phenotypic integration in the laboratory rat. Evolution 42: 28–41.

Zelditch ML, Swideresky DL, Sheets HD, Fink WL. 2004. Geometric morphometric for biologists. London: Elsevier Academic Press.